



Published in final edited form as:

*Leukemia*. 2016 May ; 30(5): 1033–1043. doi:10.1038/leu.2015.353.

## CDK6-mediated repression of CD25 is required for induction and maintenance of Notch1- induced T cell acute lymphoblastic leukemia

Nilamani Jena<sup>1,2</sup>, Jinghao Sheng<sup>1</sup>, Jamie K. Hu<sup>1</sup>, Wei Li<sup>1</sup>, Wenhui Zhou<sup>1</sup>, Gene Lee<sup>1</sup>, Nicolaos Tsihchlis<sup>1</sup>, Aparna Pathak<sup>1</sup>, Nelson Brown<sup>1</sup>, Amit Deshpande<sup>1</sup>, Chi Luo<sup>1</sup>, Guo-fu Hu<sup>1</sup>, Philip W. Hinds<sup>1,3</sup>, Richard A. Van Etten<sup>1,2</sup>, and Miaofen G. Hu<sup>1,\*</sup>

<sup>1</sup>Molecular Oncology Research Institute, Tufts Medical Center, Boston, MA 02111, USA

### Abstract

T-cell acute lymphoblastic leukemia (T-ALL) is a high-risk subset of acute leukemia, characterized by frequent activation of Notch1 or AKT signaling, where new therapeutic approaches are needed. We showed previously that Cyclin-dependent kinase 6 (CDK6) is required for thymic lymphoblastic lymphoma induced by activated AKT. Here, we show CDK6 is required for initiation and maintenance of Notch-induced T-ALL. In a mouse retroviral model, hematopoietic stem/progenitor cells lacking CDK6 protein or expressing kinase-inactive (K43M) CDK6 are resistant to induction of T-ALL by activated Notch, whereas those expressing INK4-insensitive (R31C) CDK6 are permissive. Pharmacologic inhibition of CDK6 kinase induces CD25 and RUNX1 expression, cell cycle arrest, and apoptosis in mouse and human T-ALL. Ablation of *Cd25* in a K43M background restores Notch-induced T-leukemogenesis, with disease that is resistant to CDK6 inhibitors in vivo. These data support a model whereby CDK6-mediated suppression of CD25 is required for initiation of T-ALL by activated Notch1, and CD25 induction mediates the therapeutic response to CDK6 inhibition in established T-ALL. These results both validate CDK6 as a molecular target for therapy of this subset of T-ALL and suggest that CD25 expression could serve as a biomarker for responsiveness of T-ALL to CDK4/6 inhibitor therapy.

---

Users may view, print, copy, and download text and data-mine the content in such documents, for the purposes of academic research, subject always to the full Conditions of use: [http://www.nature.com/authors/editorial\\_policies/license.html#terms](http://www.nature.com/authors/editorial_policies/license.html#terms)

\*Correspondence: Miaofen G. Hu, M.D., Ph.D., Molecular Oncology Research Institute, Tufts Medical Center 800 Washington Street Box 5609, Boston, MA 02111, Tel: 617-636-4929, Fax: 617-636-9230, ; Email: [mhu@tuftsmedicalcenter.org](mailto:mhu@tuftsmedicalcenter.org)

<sup>2</sup>Current address: Chao Family Comprehensive Cancer Center, University of California Irvine, 839 Medical Sciences Court, Sprague Hall Room 124, Irvine CA 92697

<sup>3</sup>Current address: Tufts University School of Medicine, 150 Harrison Avenue, Boston, MA 02111

### Authorship

Contribution: N.J. designed and performed experiments, analyzed data, interpreted results; J.S., J.K.H., W. L., W.Z., G.L., N.T., A.P., N.B., A.D., and C.L. assisted in genotyping and performed experiments; G.F.H. and P.W.H. provided guidance and reagents; R.V.E. provided guidance for the group and assisted in manuscript preparation; and M.G.H. designed and performed experiments, interpreted results, provided guidance for the group, and wrote the manuscript.

**Conflict-of-interest disclosure:** The authors declare no competing financial interests.

## Introduction

T-cell acute lymphoblastic leukemia (T-ALL) is a malignancy of immature T lymphocytes treated with complex combination chemotherapy that is generally effective at inducing remission of the disease. However, a high proportion of T-ALL patients suffer relapse, possibly because the available therapies do not eradicate leukemic stem cells (LSCs) that initiate and sustain the disease. Treatment options for patients with relapsed or refractory T-ALL are limited. Agents such as nelarabine and clofarabine induce responses in <20% of patients. It is thus imperative to develop new therapies for T-ALL directed against specific targets in leukemic cells.<sup>1</sup> More than half of T-ALLs have activating *NOTCH1* mutations<sup>2-4</sup> or abnormalities in the PTEN-AKT pathways.<sup>5,6</sup> Small-molecule gamma-secretase inhibitors (GSIs), which block a critical proteolytic step required for NOTCH1 activation, have activity against T-ALLs with NOTCH1 mutations but not those with *PTEN* deficiency or constitutively active AKT.<sup>5</sup> The clinical development of GSIs in T-ALL has been hampered by gastrointestinal toxicity, while therapeutic responses to GSIs are modest and transient.<sup>7</sup> In addition to acquired loss-of-function mutations in *PTEN*,<sup>5,8</sup> GSI resistance may also develop in a small subset of primary T-ALL cells through BRD4-dependent epigenetic chromatin modifications that sustain expression of several NOTCH target genes, including *MYC*, *BCL2*, and *CDK6*.<sup>9</sup> To improve the efficacy of human T-ALL therapy, it is necessary to inhibit both the Notch and PTEN pathways or to target a common downstream effector. It would also be desirable to identify additional biomarkers for predicting response to targeted therapy, since all patients with T-ALL are currently treated similarly regardless of the underlying pathogenesis.

Cyclin-dependent kinase 6 (CDK6) regulates the G<sub>1</sub>-S phase transition by phosphorylating the retinoblastoma protein (pRB).<sup>10</sup> It also binds to RUNX1 and promotes its degradation,<sup>11</sup> thereby playing a cell cycle-independent role. There is currently much interest in CDK6 and the closely related CDK4 kinase as targets for cancer therapy. CDK4 is required for breast carcinogenesis in a mouse model,<sup>12</sup> and the CDK4/6 inhibitor palbociclib (PD0332991) was recently approved by the U.S. Food and Drug Administration for treatment of women with estrogen receptor-positive, human epidermal growth factor receptor-negative metastatic breast cancer in combination with the aromatase inhibitor letrozole. In T-lymphoid malignancies, Cyclin D2 is dysregulated via chromosomal translocations in a subset of T-ALL,<sup>13</sup> whereas CDK6 is over-expressed in T-ALL cells<sup>14</sup> and the *CDK6* locus amplified in a quarter of peripheral T-cell lymphomas.<sup>15</sup> Two recent studies have shown that a CDK4/6 inhibitor can block proliferation and induce apoptosis in mouse T-ALLs induced by activated Notch1,<sup>16,17</sup> but the relevant CDK target and molecular mechanisms involved were not defined.

To address the role of CDK6 kinase activity in development and tumorigenesis, we have produced both knockout (*KO*) and knock-in mice by introducing a LoxP-flanked transcriptional STOP cassette into intron 1 of the *Cdk6* gene adjacent to the intact /mutant exon 1.<sup>18,19</sup> In the presence of the STOP cassette CDK6 expression is prevented, resulting in a null allele (*Cdk6*<sup>-/-</sup> or *KO*). Upon excision of the cassette by CRE recombinase, the CRE-reactivated wild-type allele or the mutant alleles express WT or mutant CDK6, respectively, from the endogenous locus with intact regulatory controls. The knock-in mutants include

CDK6<sup>R31C</sup> (R31C), a hyper-active, inhibitor-resistant kinase that cannot interact with INK4 family inhibitor proteins,<sup>20</sup> and a catalytically inactive kinase, CDK6<sup>K43M</sup> (K43M).<sup>19</sup> The R31C mutant mimics hyperactivation of CDK6 in tumor cells, whereas the catalytic inactive K43M mutant models pharmacological inhibition of kinase activity.

Our previous studies demonstrated that that CDK6 is required for thymocyte development and for precursor T cell lymphoma induced by activated AKT.<sup>18,19</sup> Here, we tested the role of CDK6 kinase activity in T-ALL and demonstrate that CDK6-mediated repression of CD25,  $\alpha$ -chain of IL2R, is required for induction of T-ALL by activated Notch, whereas induction of CD25 mediates the therapeutic response to CDK6 inhibition in established T-ALL. These studies validate CDK6 as a therapeutic target in human T-ALL and suggest that CD25 expression could serve as a biomarker for response of T-ALL patients to a CDK6 inhibitor.

## Materials and Methods

### Mice

Generation of different *Cdk6* mutant mice and *K43M;Cd25<sup>-/-</sup>* mice has been published.<sup>18,19</sup> We backcrossed mice bearing the *KO*, *R31C* and *K43M* alleles eight times to C57BL/6. All experiments were performed according to the guidelines of the Institutional Animal Care and Use Committee of Tufts Medical School.

To induce specific deletion of *Runx1* or *Rb* in thymocytes, we crossed *Runx1<sup>fl/fl</sup>* or *Rb<sup>fl/fl</sup>* and *K43M;Runx1<sup>fl/fl</sup>* or *K43M;Rb<sup>fl/fl</sup>* mice with *LCK-Cre* transgenic mice to induce specific deletion of *Runx1* or *Rb*. Lack of RUNX1/RB expression in the thymocytes was confirmed by PCR using primers described<sup>21,22</sup> and by Western blotting.

### Virus

MigR1 retroviral vectors expressing ICN-GFP or ICN-DsRed were kindly provided by Drs. Jon Aster (Brigham and Women's Hospital, Boston, Massachusetts) and Harald von Boehmer (Dana-Farber Cancer Institute, Boston, Massachusetts), respectively. We constructed retroviral expression vectors (MigR1-ICN-CRE-GFP) co-expressing active Notch (ICN) with a GFP-CRE fusion protein.<sup>23</sup> We also constructed a retroviral expression vector (MigR1-GFP-CDK6) carrying the mouse *Cdk6* cDNA.

### Induction of Notch-induced leukemia by retroviral transduction and transplantation

We induced Notch-induced leukemia by retroviral gene transfer as described.<sup>24,25</sup> We isolated Lin<sup>-</sup>Kit<sup>+</sup> (LK) BM cells by flow cytometry and transduced them twice by spin infection with high-titer, helper-free replication-defective ICN retrovirus stock. We injected retrovirally transduced GFP<sup>+</sup> cells (~ 3 x 10<sup>5</sup>) via tail vein into sub-lethally irradiated C57B6 recipients. We monitored the recipients for disease by analyzing peripheral blood or different tissues, including thymus, spleen, BM and LN, for the presence of CD4<sup>+</sup>CD8<sup>+</sup> double-positive (DP) cells. For double retroviral transduction experiments as described in Fig. 3, isolated K43M-LK cells were transduced with ICN-IRES-DsRed virus (ICN-DsRed) together with either with *Cdk6*-IRES-GFP (CDK6-

GFP) or IRES-GFP (GFP) virus by spin infection.  $\sim 3 \times 10^5$  cells ( $\sim 10\text{--}15\%$  transduction efficiency of double-transduced cells) that expressed both DsRed and GFP were isolated by flow sorting and injected into sub-lethally irradiated C57B6 recipients.

### Drug treatment

For *in vivo* treatment with LEE011, we induced T-ALL by injecting  $10^6$  leukemic cells derived from WT-ICN, Cd25<sup>-/-</sup>-ICN, and K43M;Cd25<sup>-/-</sup>-ICN leukemic mice into sub-lethally irradiated C57B6 recipients via tail vein. The recipients were treated with LEE011 (200 mg/kg daily by gavage) or vehicle (0.5% methycellulose) for 46 days beginning 2 weeks post-transplantation when GFP<sup>+</sup> cells were detected in the peripheral blood. After 7 days of treatment, we collected cells from blood to analyze apoptosis, cell cycle composition, and expression level of CD25 by FACS analysis using staining with Annexin V, 7AAD, PI, and anti-CD25 antibody and by Western Blotting using apoptosis marker Cleaved Caspase 3 (#9664, CST).

### Statistical methods

For most experiments, the sample size was chosen based on expected differences between experimental and control groups in order to provide adequate power to detect a significant difference specifying  $\alpha = 0.05$ , two-tailed testing, and power ( $= 1 - \beta$ ) of 80%, using commercially available software packages (Statistical Solutions nQuery Advisor; <http://www.statsol.ie/nquery/nquery.htm>). For transplantation experiments, our control cohorts are typically designed to have fairly tight incidence curves, allowing the experiment to be adequately powered with recipient cohorts of  $n = 8\text{--}12$  subjects. For animal experiments, because of the total absence of leukemia phenotypes in *Cdk6* loss-of-function backgrounds, operator blinding was not feasible.

## Results

### CDK6 kinase activity is required for induction of T-ALL by activated Notch1

To determine if CDK6 kinase activity is required for T-cell transformation by activated Notch, we used a mouse retroviral leukemia model.<sup>24</sup> We sorted hematopoietic Lin<sup>-</sup>c-Kit<sup>+</sup> (LK) stem/progenitor cells from bone marrow (BM) of *WT*, *KO*, *K43M*, and *R31C* mice and transduced the sorted cells with retrovirus expressing the activated, intracellular form of human Notch1 (ICN) together with GFP (Supplementary Figure S1a). Consistent with previous reports<sup>24</sup>, transduction of *WT/R31C* LK cells with activated ICN1 led to appearance of T-ALL, manifested by CD4<sup>+</sup>CD8<sup>+</sup> double-positive (DP) T cells in 100% of recipient mice. Gross and microscopic examination (Figure 1a and Supplementary Figure S1b) showed that *WT-ICN1/R31C-ICN* but not *KO-ICN1* and *K43M-ICN1* recipient mice had markedly enlarged spleen, thymi (data not shown), lymph nodes (LN), and liver (data not shown), due to extensive infiltration of organs by cells morphologically consistent with lymphoblasts.<sup>24</sup> The circulating white blood cells (WBC) in each of the *WT-ICN1* and *R31C-ICN1* recipient mice increased 5–7 weeks post-BMT to  $26\text{--}72 \times 10^3/\mu\text{l}$  (normal range:  $1.8\text{--}10 \times 10^3/\mu\text{l}$ ), as did the number of GFP<sup>+</sup> splenocytes (Supplementary Figure S1c). As expected, all animals became moribund by 8 weeks post-BMT (Figure 1b). Flow cytometry confirmed the presence of GFP<sup>+</sup>-DP T cells in thymi, blood, and spleen (Figure

1c). Similar results were also found in analyses of cells isolated from BM, and lymph nodes from each mouse (data not shown). GFP<sup>+</sup> cells were further confirmed to express Thy1/CD90 (Supplementary Figure S1d), but not markers for other hematopoietic lineages such as granulocytes, macrophages, and B cells (Supplementary Figure S1e–g). In contrast, none of *KO*-ICN or *K43M*-ICN recipients had detectable GFP<sup>+</sup> DP/CD90<sup>+</sup> cells in thymus, blood, and spleen during the observation period or at necropsy at 20 weeks post-BMT. Together, these data demonstrate CDK6 kinase activity is required for Notch1 to transform hematopoietic progenitors.

Transplantation (intravenous via tail vein) of 10<sup>6</sup> whole BM cells from primary recipients of *WT*-ICN or *R31C*-ICN progenitors resulted in rapidly fatal T-ALL in secondary recipients, whereas similar transplants from *KO*-ICN and *K43M*-ICN recipients failed to induce leukemia (data not shown). This suggests that CDK6 is required for maintenance of leukemia-initiating cells in recipients of ICN-transduced stem/progenitor cells, as assessed by serial transplantation.

### Loss of CDK6 kinase activity impairs the survival and proliferation of *K43M*-ICN progenitors

The defect in Notch1-induced leukemogenesis in *KO* and *K43M* donor cells was not due to inefficient retroviral transduction (Supplementary Figure S2a) or impaired homing to recipient BM and spleen following transplantation (Supplementary Figure S2b–c). At three weeks post-transplant when GFP<sup>+</sup> cells but not DP cells were still detectable in the peripheral blood (data not shown) and spleen (Supplementary Figure S2d–e) of *K43M*-ICN recipients, there was a marked reduction in the S/G2/M phase and an increase in the G<sub>1</sub> and sub-2n populations in GFP<sup>+</sup> splenocytes of *K43M*-ICN recipients relative to those of *WT*-ICN recipients (Figure 2a). Flow cytometric analysis revealed that GFP<sup>+</sup> splenocytes from *K43M*-ICN recipients had significantly increased apoptosis compared with those from *WT*-ICN recipients (Figure 2b), which was confirmed by increased levels of activated, cleaved Caspase-3 (Figure 2c).<sup>26,27</sup> Expression of ICN, albeit at lower levels than in *WT*-ICN recipients, confirmed the presence of retrovirally-transduced cells in the GFP<sup>+</sup> *K43M*-ICN splenocyte population. The lower levels of ICN expression in retrovirally transduced *K43M* progenitors motivated the examination of endogenous Notch1 levels in thymocytes. Lack of CDK6 or its kinase activity in thymocytes resulted in reduced levels of extracellular Notch1 protein, whereas constitutively active CDK6 (*R31C*) was associated with increased intracellular Notch1 (Supplementary Figure S2f), suggesting an autoregulatory feedback of CDK6 on Notch1 levels and signaling. Together, these results suggest that loss of CDK6 kinase activity results in enhanced apoptosis and an impaired proliferative response of T cell progenitors to activated Notch.

### Re-expression of CDK6 in *KO* or *K43M* LK cells rescues the defect in leukemogenesis

To demonstrate that the failure of ICN to induce T-ALL from *KO* and *K43M* BM is indeed due to CDK6 deficiency and not a consequence of decreased frequency or function of a particular BM target cell for transduction by the ICN retrovirus, we restored CDK6 expression in *KO* donor LK cells using a MigR1 retrovirus expressing a GFP-CRE (CRE) fusion protein,<sup>23</sup> either alone (CRE) or with together with ICN (ICN-CRE) to remove the

STOP cassette in the *Cdk6* conditional null allele<sup>18</sup> (Supplementary Figure S3a–b) in transduced cells. We first assessed the efficacy of CRE-induced restoration of CDK6 expression in *KO* mouse embryonic fibroblasts. CDK6 expression was successfully restored after transduction with CRE or ICN-CRE retrovirus, whereas ICN was simultaneously expressed in cells infected with ICN-CRE (Supplementary Figure S3c).

*KO* progenitors transduced with ICN-CRE induced T-ALL as efficiently as transduced *WT* LK cells (Figure 3a, left panel), characterized by organomegaly (Supplementary Figure S3d–g) and splenic infiltration with GFP<sup>+</sup>CD4<sup>+</sup>CD8<sup>+</sup>CD90<sup>+</sup> leukemic cells (Figure 3b, left panel and Supplementary Figure S3h). By contrast, *KO*-LK cells transduced with CRE or with ICN alone failed to develop T-ALL (Figure 3a–b, left panels and Supplementary Figure S3e–f). Expression of CDK6 and ICN in leukemic blasts from spleen was comparable between leukemias derived from ICN-CRE-transduced *WT* or *KO* progenitors (Figure 3c, left panel).

We also re-expressed CDK6 with ICN in *K43MLK* cells by dual transduction with MigR1 retroviruses individually expressing ICN (ICN-IRES-DsRed; ICN-DsRed)<sup>28</sup> and CDK6 (*Cdk6*-IRES-GFP; CDK6-GFP). *K43M*-LK cells transduced with both ICN-DsRed and CDK6-GFP viruses induced fatal T-ALL, while *K43M*-LK cells transduced with ICN-DsRed and control vector (V-GFP) retroviruses failed to induce TALL (Figure 3a, right panel). Leukemic mice displayed organomegaly (Supplementary Figure S3i) and organ infiltration with GFP<sup>+</sup>DsRed<sup>+</sup> lymphoblasts (Supplementary Figure S3j) with a mixed CD4<sup>+</sup>SP and DP immunophenotype (Figure 3b, right panel) rather than the predominantly DP lymphoblasts observed in a *WT* background (Figure 1c). Splenocyte CDK6 protein levels in recipients of ICN-DsRed+CDK6-GFP-transduced *K43M* progenitors were significantly higher than those of ICN-DsRed+V-GFP recipients (Figure 3c, right panel). Taken together, these data indicate that re-expression of CDK6 in *KO* or *K43MLK* cells rescues the defect in leukemogenesis.

### Ablation of *Cd25* restores the ability of *K43M* LK cells to induce leukemogenesis

The higher levels of CD25 observed in *KO* and *K43M* thymocytes indicate that CDK6 kinase activity is essential to down-regulate CD25 expression during normal thymocyte development.<sup>18,19</sup> To determine the role of CD25 in Notch-mediated transformation, we isolated LK cells from *K43M*, *CD25*<sup>-/-</sup>, and *K43M;Cd25*<sup>-/-</sup>, and *WT* donors and induced T-ALL as described above. Lack of CD25 expression in leukemic (GFP<sup>+</sup>) cells was confirmed by PCR (data not shown) and by flow cytometric analysis (Supplementary Figure S4a–c). All *Cd25*<sup>-/-</sup>-ICN and *Cd25*<sup>-/-</sup>;*K43M*-ICN recipients developed T-ALL. By 9 weeks post-transplant, all *Cd25*<sup>-/-</sup>-ICN and *K43M;Cd25*<sup>-/-</sup>-ICN recipients (Figure 4a) became moribund with a median survival of 53 days, which was not significantly different from that of *WT*-ICN recipients (58 days). The immunophenotype of T-ALL in *Cd25*<sup>-/-</sup>-ICN and *K43M;Cd25*<sup>-/-</sup>-ICN recipients (Figure 4b and Supplementary Figure S4d) was similar to that of *WT*-ICN recipients (GFP<sup>+</sup>CD4<sup>+</sup>CD8<sup>+</sup>CD90<sup>+</sup>). These results demonstrate that ablation of *Cd25* sensitizes *K43MLK* cells to ICN-mediated transformation and suggest that CDK6-mediated repression of CD25 is required for Notch-induced T-ALL.

## Neither pRB nor RUNX1 is the effector that mediates CDK6-dependent repression of CD25 and sensitivity to Notch transformation

To investigate how alterations of CDK6 kinase activity may affect, at the molecular and cellular levels, Notch signaling in thymocyte development and transformation, we first explored if pRB, a known substrate of CDK6, mediates the effect of CDK6 on thymocyte CD25 expression. *K43M;Rb1<sup>fl/fl</sup>* mice were crossed with *LCK-Cre* transgenic mice to induce specific deletion of *Rb1* in thymocytes (Supplementary Figure S5a). Consistent with a previous study,<sup>17</sup> deletion of *Rb1* in the *K43M* background partially rescued some of the thymocyte defects seen in *K43M* mice, such as total thymocyte cellularity (Supplementary Figure S5b). However, CD25 expression levels were similar in DN thymocytes from *K43M* and *K43M;Rb1<sup>fl/fl</sup>;LCK-Cre* mice and from *WT* and *Rb1<sup>fl/fl</sup>;LCK-Cre* mice (Supplementary Figure S5c), indicating that regulation of CD25 expression by CDK6 is independent of pRB.

We also tested whether RUNX1, a transcription factor implicated in regulation of *Cd25*,<sup>29,30</sup> that is phosphorylated by CDK6 on serine 303 and subsequently destabilized<sup>11,31</sup> might serve as a downstream effector for CDK6. To determine if RUNX1 mediates CDK6-mediated repression of CD25, we generated *K43M;Runx1<sup>fl/fl</sup>* mice and then crossed *Runx1<sup>fl/fl</sup>* and *K43M;Runx1<sup>fl/fl</sup>* with *LCK-Cre* mice to induce specific deletion of *Runx1* in thymocytes. Compared to *WT* thymocytes, *K43M* thymocytes had higher levels of RUNX1 protein but lower levels of phosphorylated RUNX1pS303 (Supplementary Figure S5d), suggesting that CDK6 is the principal kinase mediating RUNX1 phosphorylation and destabilization in response to Notch signaling.<sup>11</sup> Consistent with previous observations,<sup>32,33</sup> loss of RUNX1 reduced thymocyte number by ~40% (Supplementary Figure S5e). However, deletion of *Runx1* in the *K43M* background did not rescue the reduced thymocyte cellularity seen in *K43M* mice (Supplementary Figure S5e). Moreover, deletion of RUNX1 did not affect the level of CD25 expression, comparing either between *WT* and *Runx1<sup>fl/fl</sup>;LCK-Cre* mice or between *K43M* and *K43M;Runx1<sup>fl/fl</sup>;LCK-Cre* mice (Supplementary Figure S5f), indicating that regulation of thymocyte CD25 expression by CDK6 is independent of RUNX1.

To test whether deficiency of either pRB or RUNX1 would substitute for loss of CD25 in rescuing leukemogenesis in *K43M* progenitors, we transduced LK cells from *K43M;Rb1<sup>fl/fl</sup>* and *K43M;Runx1<sup>fl/fl</sup>* donors with ICN-CRE retrovirus and transplanted the progenitors into irradiated recipients. Neither *Rb1* nor *Runx1* deletion restored T-leukemogenesis in the *K43M* background (Supplementary Figure S5g–h), despite efficient deletion of the *Runx1<sup>fl/fl</sup>* allele by the ICN-CRE retrovirus in a *Cdk6 WT* background (Supplementary Figure S5i).

The forkhead transcription factor FOXM1 is highly expressed in Jurkat cells<sup>34</sup> and inhibition of FOXM1 increases chemosensitivity to doxorubicin in T-ALL.<sup>35</sup> Recently, CDK6 was shown to phosphorylate FOXM1, leading to stabilization of FOXM1 protein levels and stimulation of transcriptional activation.<sup>36</sup> Consistent with this, we found that KO/*K43M* thymocytes had lower FOXM1 levels than *WT/R31C* thymocytes (Supplementary Figure S5j), whereas expression levels of CD25 are higher in KO/*K43M* thymocytes and lower in *WT/R31C* thymocytes.<sup>18,19</sup> Similarly, palbociclib treatment reduced the level of FOXM1 protein in human HPBALL cells (Supplementary Figure S5k). These data suggest that

FOXM1 is potential regulator of CD25 expression downstream of CDK6 in normal and neoplastic thymocytes.

### CD25 mediates the therapeutic response to CDK6 inhibition in established T-ALL

To determine if CDK6 is a therapeutic target in established T-ALL, we treated ICN-induced mouse TALLs with LEE011 (LEE), a clinically relevant small molecule inhibitor of CDK4 and CDK6 kinases,<sup>37</sup> for 46 days beginning 2 weeks post-transplantation when GFP<sup>+</sup> cells were first detected in the blood. After 7 days of LEE treatment, *WT*-ICN recipients had a dramatic reduction in frequency of circulating GFP<sup>+</sup> leukemic cells (Figure 5a, left panel and Supplementary Figure S6a) with increased apoptosis (Figure 5a, middle panel and Supplementary Figure S6b). Leukemic cells from these mice demonstrated a prominent G<sub>1</sub> cell cycle arrest with an increased sub-G<sub>1</sub> population (Figure 5a, right panel and Supplementary Figure S6c), suppression of pRB phosphorylation at S780 and induction of cleaved Caspase-3 (Figure 5b), accompanied by increased expression of CD25 (Figure 6a). In striking contrast, both *Cd25*<sup>-/-</sup> and *K43M;Cd25*<sup>-/-</sup> recipients had little or no response to LEE treatment *in vivo*, manifested by persistence of circulating leukemic cells (Figure 5a, left panel and Supplementary Figure S6a), and no effect of the drug on apoptosis (Figure 5b, middle panel and Supplementary Figure S6b), cell cycle (Figure 5c, right panel and Supplementary Figure S6c), or phosphorylation of pRB and cleaved Caspase-3 (Figure 5b) in the malignant cells. Continuous treatment with LEE led to a dramatic improvement in survival of *WT*-ICN recipients, with 7/8 recipients remaining alive and apparently healthy at 60 days post BMT, whereas all recipients of *WT*-ICN transplants treated with vehicle became moribund by 30 days post-transplant with a median survival of ~23 days (Figure 6b, left panel). Vehicle-treated *Cd25*<sup>-/-</sup>-ICN recipients had a similar median survival of ~20 days, while there was a modest but statistically significant improvement in survival of LEE-treated *Cd25*<sup>-/-</sup>-ICN recipients (median survival ~30 days; Figure 6b, middle panel). In contrast, *K43M;Cd25*<sup>-/-</sup>-ICN recipients had virtually no response to LEE treatment, with a median survival of ~18 days for V-treated and 22.5 days for LEE-treated recipients (Figure 6b, right panel). Collectively, these results indicate that CDK6 kinase activity is required for T-ALL maintenance, as inhibition of CDK4/6 blocks cell proliferation, increases CD25 expression, and induces apoptosis. Loss of CD25 overrides the requirement for CDK6 kinase activity for Notch-mediated transformation, and renders the resulting leukemias insensitive to inhibition of CDK4/6.

### Inhibition of CDK6 kinase activity up-regulates CD25 and RUNX1 in human T-ALL cells

To extend our findings to human leukemia, we tested the response of four human T-ALL cell lines with constitutive active *Notch1* mutations<sup>2</sup> to the CDK4/6 kinase inhibitor PD0332991 (PD; palbociclib).<sup>38</sup> PD treatment inhibited cell proliferation in all four cell lines, ranging from ~4- to 14-fold reduction in the S/G<sub>2</sub>/M fraction and ~40–90% increase in G<sub>1</sub> (Figure 7a). PD treatment also induced CD25 expression in these GSI-sensitive T-ALL cells, with a ~4- to 26-fold increase in the CD25<sup>+</sup> population (Figure 7b). Similarly, PD treatment also induced CD25 expression in 5 out of 6 T-ALL cells with WT Notch receptors<sup>39</sup>, with a ~1.4 to 8-fold increase in the CD25<sup>+</sup> population (Supplementary Figure S7a–b), accompanying with inhibition of cell proliferation and increased dead cells (Supplementary Figure S7c–d). RUNX1 protein levels were also increased upon PD treatment (Figure 7c, left panel),



whereas phospho-pRB S780 and phospho-RUNX1 S303 were reduced (Figure 7c, middle panel). Moreover, PD treatment increased the level of total and CDK6-bound RUNX1 (Figure 7c, right panel). These results demonstrate that CDK6 regulates proliferation and represses RUNX1 and CD25 in Notch-mutant human T-ALL.

Whereas PD also inhibits CDK4 activity,<sup>40</sup> we used *Cdk6*-specific shRNA to examine the specific role of CDK6 in Notch-mutant human T-ALL. In HPBALL cells, CDK6 was effectively knocked down by two previously validated *Cdk6*-shRNAs<sup>41</sup> leading to dramatic hypo-phosphorylation of pRB at S780 and RUNX1 at S303, respectively, upregulation of RUNX1 protein level (Figure 8a), upregulation of CD25 protein level (Figures 8b), and inhibition of proliferation (Figures 8c). Importantly, these changes were observed despite continuous expression of CDK4 (Figure 8a). Thus, CDK6 is specifically required for phosphorylation of pRB and RUNX1 and for suppression of RUNX1 and CD25 expression in human TALL.

## Discussion

We have shown previously that CDK6 is required for T-lymphomagenesis by activated AKT.<sup>18</sup> Here, we demonstrate a previously unrecognized yet critical role of CDK6 in mediating Notch-induced T-ALL. We have provided compelling genetic, physiological, histological, cellular and molecular evidence to demonstrate that CDK6 kinase activity is critical to induction of T-ALL by activated Notch1 in a mouse model. Donor cells lacking CDK6 protein or kinase activity are resistant to transformation by activated Notch as a consequence of reduced proliferation and increased apoptosis, effects also induced by CDK4/6 inhibitor treatment *in vivo*. Re-expression of CDK6 in *Cdk6*-deficient stem cells rescues this defect, arguing for a direct role of CDK6 downstream of Notch in leukemogenesis.

Interestingly, the elevated CDK6 kinase activity in *R31C* progenitors did not result in increased aggressiveness of leukemia (as assessed by survival), possibly because increased apoptosis in *R31CLSK* cells<sup>19</sup> offset the increase in proliferation, or because increased p16INK4a in *R31CLSK* cells bound to and inhibited CDK4, partially opposing the effect of CDK6 hyperactivation.<sup>42</sup> In complementary studies, others have shown that deletion of cyclin D3 (an activating partner of CDK4/6) or treatment with palbociclib induced cell cycle arrest and apoptosis in mouse T-ALLs induced by activated Notch1 and prolonged survival of mice bearing these leukemias.<sup>17,16</sup> As more than half of T-ALL patients have either Notch or AKT mutations, the fact that Notch and PI3K-AKT signaling pathways share CDK6 as a common effector suggests a novel and highly selective therapeutic strategy against T-ALLs. Interestingly, we observed an inverse relationship between CDK6 and CD25. CD25 expression is significantly higher in the thymocytes of *KO* and *K43M* mice.<sup>19</sup> Genetic deletion of *Cd25* rescues most of the phenotypic defects in LSK production and early T cell development caused by loss of CDK6 kinase activity,<sup>19</sup> and restored T-leukemogenesis by activated Notch1 in the *K43M* background, underscoring an important role for CD25 in modulating the requirement for CDK6 kinase activity in Notch-induced T-leukemogenesis. Consistent with this, CDK6 inhibition induced CD25 expression in mouse and human TALL cells harboring activated Notch1. Furthermore, CD25<sup>+</sup> T-ALL cells were sensitive to CDK6

inhibition *in vivo*, whereas CD25-deficient T-ALLs were insensitive even though CDK6 was expressed. Interestingly, the survival of CD25<sup>-/-</sup>-ICN recipients treated with CDK4/6 inhibitor was modestly prolonged relative to vehicle-treated controls, suggesting that CD25 repression explains only part of the role of CDK6 in Notch1-driven T-ALL. Taken together, these data argue for a novel tumor suppressor role for CD25 in this genetic context, whereby ICN requires active CDK6 to downregulate CD25 for induction of T-ALL, and induction of CD25 mediates the therapeutic response to CDK6 inhibition in TALL. This, in turn, suggests that the baseline level of expression of CD25 and the CD25 response to short-term inhibition of CDK6 kinase activity could serve as a valuable biomarker for predicting the clinical response of human T-ALLs to a CDK4/6 inhibitor. Interestingly, CD25 was recently identified as a potential biomarker for response of a high-risk subset of acute myeloid leukemia to PIM inhibitors.<sup>43</sup>

The precise mechanism of regulation of CD25 levels by CDK6 is under investigation. We observed an inverse relationship between CDK6 and RUNX1 in mouse and human T-ALL, suggesting that activated Notch downregulates *Runx1*, which is also repressed by TLX1/TLX3 transcription factors and functions as a tumor suppressor in some T-ALLs.<sup>44,45</sup> However, RUNX1 is not an effector of CDK6 in modulating CD25 expression or leukemogenesis by activated Notch. Therefore, loss of RUNX1 may contribute to the pathogenesis of T-ALL in a CD25-independent manner, perhaps via decreased expression of PKC $\theta$  and reactive oxygen species.<sup>46</sup> Similarly, knockout of pRB does not alter CD25 expression nor does it rescue the defects in Notch-induced leukemogenesis associated with loss of CDK6 kinase activity, although deletion of pRB partially restores the development of *K43M* thymocytes. Another potential effector of CD25 expression downstream of CDK6 is FOXM1. Consistent with the observation that CDK4/6 stabilize and activate FOXM1 by phosphorylation,<sup>36</sup> we confirmed that deficiency of CDK6 kinase activity is associated with decreased FOXM1 protein levels in thymocytes. Whereas FOXM1 is generally considered a transcriptional activator, in breast cancer FOXM1 negatively regulates mammary differentiation by promoting methylation of the *GATA3* promoter and thus repressing this key regulator of luminal differentiation.<sup>47</sup> We showed previously that expression of *GATA3* is higher in KO/*K43M* thymocytes but lower in WT/*R31C* cells,<sup>19</sup> and *GATA3* knockdown in differentiated T cells correlated with strong reduction of CD25 levels.<sup>19</sup> Moreover, the mouse *GATA3* promoter contains three FOXM1 consensus sequences within 2kb of the transcriptional start site,<sup>47</sup> and there are GATA factor consensus binding sequences within 1.3 kb and 4.0 kb of the transcriptional start sites of mouse<sup>48,49</sup> and human<sup>49-51</sup> *IL2RA* genes, respectively. Therefore, it is possible that CDK6 regulates CD25 expression in part through increased FOXM1-mediated repression of *GATA3*.

In the setting of mouse or human T-ALL, it is known that activation of Notch (ICN) leads to activation of CDK6 via upregulation of CDK6 and/or by increased cyclin D3 protein.<sup>52,53</sup> Phosphorylation of ICN1 by some kinases such as Cyclin C-CDK3/8/19 promotes binding of ICN1 to Fbw7, a ubiquitin ligase, which then triggers ICN1 polyubiquitylation and proteolytic degradation.<sup>52</sup> We noted that loss of CDK6 or its kinase activity in thymocytes resulted in reduction in extracellular domain of Notch1 protein, whereas constitutively activated CDK6 kinase was associated with an increase in levels of the intracellular domain

of Notch1 (ICN; Supplementary Figure S2f), although the mechanism is not known. These observations suggest that CDK6 might regulate directly the expression and activity of Notch1 and thus have a positive feedback effect on Notch1, which in turn up-regulates CDK6.<sup>53</sup>

In conclusion, our data reveal a previously unknown relationship connecting CDK6 to T-ALL through negative regulation of CD25 expression. Further studies will be required to define the mechanism through which loss of CD25 confers independence of CDK6 to Notch1-induced T-ALL. Whereas mouse and human T-ALL cells do not express a functional IL-2 receptor or respond to IL-2 stimulation, it is unlikely that IL-2 signaling per se is involved. It is possible that deletion of CD25 allows thymic precursors expression constitutively active Notch1 to differentiate further to a state where proliferation is driven by another CDK, as suggested by palbociclib-resistant pRB phosphorylation in these leukemic cells (Figure 5b). Uncovering this mechanism should reveal additional targets and strategies for pharmacological intervention in this deadly disease.

## Supplementary Material

Refer to Web version on PubMed Central for supplementary material.

## Acknowledgments

We thank Dr. Jon Aster (Brigham and Women's Hospital, Boston, MA) for MigR1-ICN retrovirus and human T-ALL cell lines, and Dr. Harald von Boehmer (Dana-Farber Cancer Institute, Boston, MA) for ICN-DsRed and DsRed-V retroviruses. We thank Dr. Michelle Kelliher (UMass Medical School) for human T-ALL cell lines with wild type Notch1 receptor. We thank Novartis Institutes for Biomedical Research (Cambridge, MA) for LEE011. This work was supported by a V Foundation Translational Research Grant, Tufts Medical Center Research Fund, a Tufts CTSI-Catalyst Award (UL1 TR001064), and Tufts University Seed Grants to M.G.H.; R01 CA090576 to R.A.V.; R01 CA127392 to P.W.H.; and R01 CA105241 and R01 NS065237 to G.F.H.

## References

1. Zhao WL. Targeted therapy in T-cell malignancies: dysregulation of the cellular signaling pathways. *Leukemia*. 2010; 24:13–21. [PubMed: 19865108]
2. Weng AP, Ferrando AA, Lee W, Morris JPt, Silverman LB, Sanchez-Irizarry C, et al. Activating mutations of NOTCH1 in human T cell acute lymphoblastic leukemia. *Science*. 2004; 306:269–271. [PubMed: 15472075]
3. Weerkamp F, van Dongen JJ, Staal FJ. Notch and Wnt signaling in T-lymphocyte development and acute lymphoblastic leukemia. *Leukemia*. 2006; 20:1197–1205. [PubMed: 16688226]
4. Mansour MR, Linch DC, Feroni L, Goldstone AH, Gale RE. High incidence of Notch-1 mutations in adult patients with T-cell acute lymphoblastic leukemia. *Leukemia*. 2006; 20:537–539. [PubMed: 16424867]
5. Palomero T, Sulis ML, Cortina M, Real PJ, Barnes K, Ciofani M, et al. Mutational loss of PTEN induces resistance to NOTCH1 inhibition in T-cell leukemia. *Nat Med*. 2007; 13:1203–1210. [PubMed: 17873882]
6. Reynolds C, Roderick JE, LaBelle JL, Bird G, Mathieu R, Bodaar K, et al. Repression of BIM mediates survival signaling by MYC and AKT in high-risk T-cell acute lymphoblastic leukemia. *Leukemia*. 2014; 28:1819–1827. [PubMed: 24552990]
7. Palomero T, Ferrando A. Therapeutic targeting of NOTCH1 signaling in T-cell acute lymphoblastic leukemia. *Clin Lymphoma Myeloma*. 2009; 9(Suppl 3):S205–210. [PubMed: 19778842]

8. Jotta PY, Ganazza MA, Silva A, Viana MB, da Silva MJ, Zambaldi LJ, et al. Negative prognostic impact of PTEN mutation in pediatric T-cell acute lymphoblastic leukemia. *Leukemia*. 2010; 24:239–242. [PubMed: 19829307]
9. Knoechel B, Roderick JE, Williamson KE, Zhu J, Lohr JG, Cotton MJ, et al. An epigenetic mechanism of resistance to targeted therapy in T cell acute lymphoblastic leukemia. *Nat Genet*. 2014; 46:364–370. [PubMed: 24584072]
10. Sherr CJ, Roberts JM. Inhibitors of mammalian G1 cyclin-dependent kinases. *Genes Dev*. 1995; 9:1149–1163. [PubMed: 7758941]
11. Biggs JR, Peterson LF, Zhang Y, Kraft AS, Zhang DE. AML1/RUNX1 phosphorylation by cyclin-dependent kinases regulates the degradation of AML1/RUNX1 by the anaphase-promoting complex. *Mol Cell Biol*. 2006; 26:7420–7429. [PubMed: 17015473]
12. Yu Q, Sicinska E, Geng Y, Ahnstrom M, Zagodzoon A, Kong Y, et al. Requirement for CDK4 kinase function in breast cancer. *Cancer Cell*. 2006; 9:23–32. [PubMed: 16413469]
13. Clappier E, Cuccuini W, Cayuela JM, Vecchione D, Baruchel A, Dombret H, et al. Cyclin D2 dysregulation by chromosomal translocations to TCR loci in T-cell acute lymphoblastic leukemias. *Leukemia*. 2006; 20:82–86. [PubMed: 16270038]
14. Chilosi M, Doglioni C, Yan Z, Lestani M, Menestrina F, Sorio C, et al. Differential expression of cyclin-dependent kinase 6 in cortical thymocytes and T-cell lymphoblastic lymphoma/leukemia. *Am J Pathol*. 1998; 152:209–217. [PubMed: 9422538]
15. Nagel S, Leich E, Quentmeier H, Meyer C, Kaufmann M, Drexler HG, et al. Amplification at 7q22 targets cyclin-dependent kinase 6 in T-cell lymphoma. *Leukemia*. 2008; 22:387–392. [PubMed: 17989712]
16. Choi YJ, Li X, Hydbring P, Sanda T, Stefano J, Christie AL, et al. The requirement for cyclin D function in tumor maintenance. *Cancer Cell*. 2012; 22:438–451. [PubMed: 23079655]
17. Sawai CM, Freund J, Oh P, Ndiaye-Lobry D, Bretz JC, Strikoudis A, et al. Therapeutic targeting of the cyclin D3:CDK4/6 complex in T cell leukemia. *Cancer Cell*. 2012; 22:452–465. [PubMed: 23079656]
18. Hu MG, Deshpande A, Enos M, Mao D, Hinds EA, Hu GF, et al. A requirement for cyclin-dependent kinase 6 in thymocyte development and tumorigenesis. *Cancer Res*. 2009; 69:810–818. [PubMed: 19155308]
19. Hu MG, Deshpande A, Schlichting N, Hinds EA, Mao C, Dose M, et al. CDK6 kinase activity is required for thymocyte development. *Blood*. 2011; 117:6120–6131. [PubMed: 21508411]
20. Pavletich NP. Mechanisms of cyclin-dependent kinase regulation: structures of Cdks, their cyclin activators, and Cip and INK4 inhibitors. *J Mol Biol*. 1999; 287:821–828. [PubMed: 10222191]
21. Chen MJ, Yokomizo T, Zeigler BM, Dzierzak E, Speck NA. Runx1 is required for the endothelial to haematopoietic cell transition but not thereafter. *Nature*. 2009; 457:887–891. [PubMed: 19129762]
22. Gutierrez GM, Kong E, Sabbagh Y, Brown NE, Lee JS, Demay MB, et al. Impaired bone development and increased mesenchymal progenitor cells in calvaria of RB1<sup>-/-</sup> mice. *Proc Natl Acad Sci U S A*. 2008; 105:18402–18407. [PubMed: 19020086]
23. Walz C, Ahmed W, Lazarides K, Betancur M, Patel N, Hennighausen L, et al. Essential role for Stat5a/b in myeloproliferative neoplasms induced by BCR-ABL1 and JAK2(V617F) in mice. *Blood*. 2012; 119:3550–3560. [PubMed: 22234689]
24. Aster JC, Xu L, Karnell FG, Patriub V, Pui JC, Pear WS. Essential roles for ankyrin repeat and transactivation domains in induction of T-cell leukemia by notch1. *Mol Cell Biol*. 2000; 20:7505–7515. [PubMed: 11003647]
25. Krause DS, Lazarides K, von Andrian UH, Van Etten RA. Requirement for CD44 in homing and engraftment of BCR-ABL-expressing leukemic stem cells. *Nat Med*. 2006; 12:1175–1180. [PubMed: 16998483]
26. Salvesen GS. Caspases: opening the boxes and interpreting the arrows. *Cell Death Differ*. 2002; 9:3–5. [PubMed: 11803369]
27. Ghavami S, Hashemi M, Ande SR, Yeganeh B, Xiao W, Eshraghi M, et al. Apoptosis and cancer: mutations within caspase genes. *J Med Genet*. 2009; 46:497–510. [PubMed: 19505876]

28. Li X, Sanda T, Look AT, Novina CD, von Boehmer H. Repression of tumor suppressor miR-451 is essential for NOTCH1-induced oncogenesis in T-ALL. *J Exp Med*. 2011; 208:663–675. [PubMed: 21464222]
29. Ono M, Yaguchi H, Ohkura N, Kitabayashi I, Nagamura Y, Nomura T, et al. Foxp3 controls regulatory T-cell function by interacting with AML1/Runx1. *Nature*. 2007; 446:685–689. [PubMed: 17377532]
30. Miyazaki K, Miyazaki M, Guo Y, Yamasaki N, Kanno M, Honda Z, et al. The role of the basic helix-loop-helix transcription factor Dec1 in the regulatory T cells. *J Immunol*. 2010; 185:7330–7339. [PubMed: 21057086]
31. Zhang L, Fried FB, Guo H, Friedman AD. Cyclin-dependent kinase phosphorylation of RUNX1/AML1 on 3 sites increases transactivation potency and stimulates cell proliferation. *Blood*. 2008; 111:1193–1200. [PubMed: 18003885]
32. Egawa T, Tillman RE, Naoe Y, Taniuchi I, Littman DR. The role of the Runx transcription factors in thymocyte differentiation and in homeostasis of naive T cells. *J Exp Med*. 2007; 204:1945–1957. [PubMed: 17646406]
33. Taniuchi I, Osato M, Egawa T, Sunshine MJ, Bae SC, Komori T, et al. Differential requirements for Runx proteins in CD4 repression and epigenetic silencing during T lymphocyte development. *Cell*. 2002; 111:621–633. [PubMed: 12464175]
34. Tufekci O, Yandim MK, Oren H, Irken G, Baran Y. Targeting FoxM1 transcription factor in T-cell acute lymphoblastic leukemia cell line. *Leuk Res*. 2015; 39:342–347. [PubMed: 25557384]
35. Wang JY, Jia XH, Xing HY, Li YJ, Fan WW, Li N, et al. Inhibition of Forkhead box protein M1 by thiostrepton increases chemosensitivity to doxorubicin in T-cell acute lymphoblastic leukemia. *Mol Med Report*. 2015; 12:1457–1464.
36. Anders L, Ke N, Hydbring P, Choi YJ, Widlund HR, Chick JM, et al. A systematic screen for CDK4/6 substrates links FOXM1 phosphorylation to senescence suppression in cancer cells. *Cancer Cell*. 2011; 20:620–634. [PubMed: 22094256]
37. Rader J, Russell MR, Hart LS, Nakazawa MS, Belcastro LT, Martinez D, et al. Dual CDK4/CDK6 inhibition induces cell-cycle arrest and senescence in neuroblastoma. *Clin Cancer Res*. 2013; 19:6173–6182. [PubMed: 24045179]
38. Dickson MA, Tap WD, Keohan ML, D'Angelo SP, Gounder MM, Antonescu CR, et al. Phase II trial of the CDK4 inhibitor PD0332991 in patients with advanced CDK4-amplified well-differentiated or dedifferentiated liposarcoma. *J Clin Oncol*. 2013; 31:2024–2028. [PubMed: 23569312]
39. O'Neil J, Grim J, Strack P, Rao S, Tibbitts D, Winter C, et al. FBW7 mutations in leukemic cells mediate NOTCH pathway activation and resistance to gamma-secretase inhibitors. *J Exp Med*. 2007; 204:1813–1824. [PubMed: 17646409]
40. Fry DW, Harvey PJ, Keller PR, Elliott WL, Meade M, Trachet E, et al. Specific inhibition of cyclin-dependent kinase 4/6 by PD 0332991 and associated antitumor activity in human tumor xenografts. *Mol Cancer Ther*. 2004; 3:1427–1438. [PubMed: 15542782]
41. Sicinska E, Aifantis I, Le Cam L, Swat W, Borowski C, Yu Q, et al. Requirement for cyclin D3 in lymphocyte development and T cell leukemias. *Cancer Cell*. 2003; 4:451–461. [PubMed: 14706337]
42. Rodriguez-Diez E, Quereda V, Bellutti F, Prchal-Murphy M, Partida D, Eguren M, et al. Cdk4 and Cdk6 cooperate in counteracting the INK4 family of inhibitors during murine leukemogenesis. *Blood*. 2014; 124:2380–2390. [PubMed: 25157181]
43. Guo Z, Wang A, Zhang W, Levit M, Gao Q, Barberis C, et al. PIM inhibitors target CD25-positive AML cells through concomitant suppression of STAT5 activation and degradation of MYC oncogene. *Blood*. 2014; 124:1777–1789. [PubMed: 25006129]
44. Della Gatta G, Palomero T, Perez-Garcia A, Ambesi-Impiombato A, Bansal M, Carpenter ZW, et al. Reverse engineering of TLX oncogenic transcriptional networks identifies RUNX1 as tumor suppressor in T-ALL. *Nat Med*. 2012; 18:436–440. [PubMed: 22366949]
45. Zhang J, Ding L, Holmfeldt L, Wu G, Heatley SL, Payne-Turner D, et al. The genetic basis of early T-cell precursor acute lymphoblastic leukaemia. *Nature*. 2012; 481:157–163. [PubMed: 22237106]

46. Giambra V, Jenkins CR, Wang H, Lam SH, Shevchuk OO, Nemirovsky O, et al. NOTCH1 promotes T cell leukemia-initiating activity by RUNX-mediated regulation of PKC-theta and reactive oxygen species. *Nat Med.* 2012; 18:1693–1698. [PubMed: 23086478]
47. Carr JR, Kiefer MM, Park HJ, Li J, Wang Z, Fontanarosa J, et al. FoxM1 regulates mammary luminal cell fate. *Cell Rep.* 2012; 1:715–729. [PubMed: 22813746]
48. Sperisen P, Wang SM, Soldaini E, Pla M, Rusterholz C, Bucher P, et al. Mouse interleukin-2 receptor alpha gene expression. Interleukin-1 and interleukin-2 control transcription via distinct cis-acting elements. *J Biol Chem.* 1995; 270:10743–10753. [PubMed: 7738013]
49. Bucher P, Corthesy P, Imbert J, Nabholz M. A conserved IL-2 responsive enhancer in the IL-2R alpha gene. *Immunobiology.* 1997; 198:136–143. [PubMed: 9442385]
50. John S, Robbins CM, Leonard WJ. An IL-2 response element in the human IL-2 receptor alpha chain promoter is a composite element that binds Stat5, Elf-1, HMG-I(Y) and a GATA family protein. *Embo J.* 1996; 15:5627–5635. [PubMed: 8896456]
51. Lecine P, Algarte M, Rameil P, Beadling C, Bucher P, Nabholz M, et al. Elf-1 and Stat5 bind to a critical element in a new enhancer of the human interleukin-2 receptor alpha gene. *Mol Cell Biol.* 1996; 16:6829–6840. [PubMed: 8943338]
52. Li N, Fassl A, Chick J, Inuzuka H, Li X, Mansour MR, et al. Cyclin C is a haploinsufficient tumour suppressor. *Nat Cell Biol.* 2014; 16:1080–1091. [PubMed: 25344755]
53. Joshi I, Minter LM, Telfer J, Demarest RM, Capobianco AJ, Aster JC, et al. Notch signaling mediates G1/S cell-cycle progression in T cells via cyclin D3 and its dependent kinases. *Blood.* 2009; 113:1689–1698. [PubMed: 19001083]

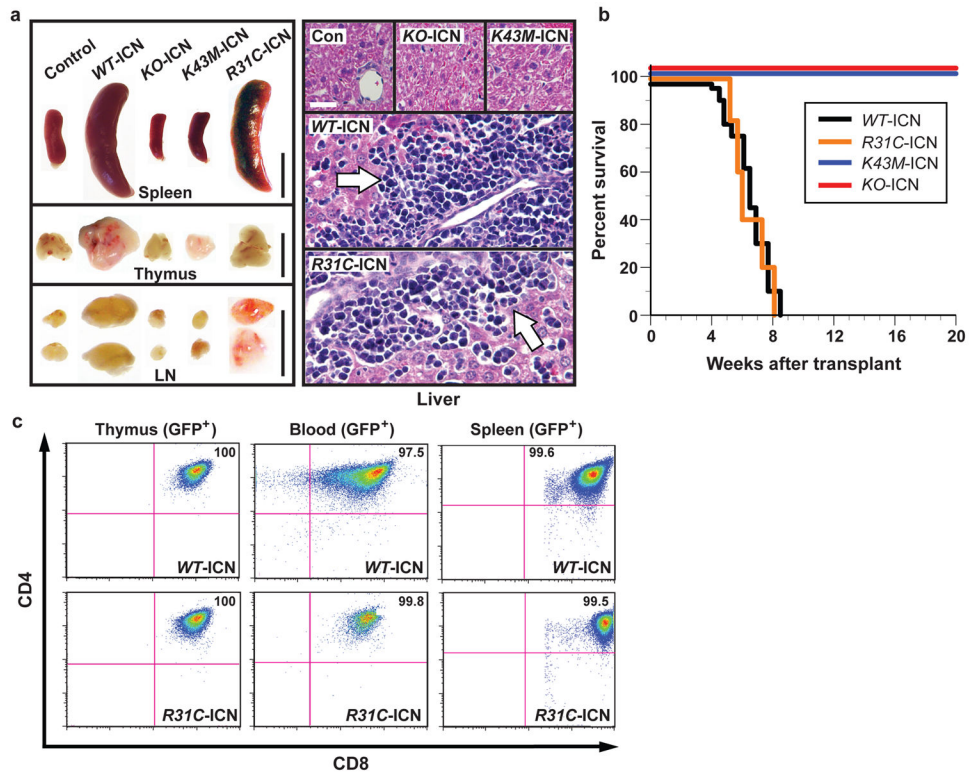


**Figure 1. CDK6 kinase activity is required for induction of T-ALL by activated Notch1**  
 (a) Left panel: representative appearance of spleen, thymus, and lymph nodes (LN) from normal (Control) mice, healthy *KO-ICN* and *K43M-ICN* recipients (8 weeks post-transplant), and moribund *WT-ICN* and *R31C-ICN* recipients (8 weeks post-transplant). The size bars on the right indicate 1 cm. Right panel: H&E staining showing leukemic blasts (indicated by white arrows) infiltrating the liver of a *WT-ICN* and *R31C-ICN* recipient but not *KO-ICN* and *K43M-ICN* recipients. A non-transplanted mouse (Con) was included as a control (scale bar: 50  $\mu$ m). (b) Kaplan-Meier survival curves for recipients of MigR1-ICN-GFP-transduced LK cells from *K43M* ( $n = 20$ ), *KO* ( $n = 10$ ), *R31C* ( $n = 5$ ), and *WT* ( $n = 20$ ) donors. The difference in survival between *WT-ICN* and *KO-ICN*, and between *WT-ICN* and *K43M-ICN*, was significant ( $P < 0.05$ , log-rank tests). (c) Flow cytometric analyses of GFP<sup>+</sup>-CD4<sup>+</sup>CD8<sup>+</sup> DP cells in thymocytes (Thy), blood, and spleen derived from moribund *WT-ICN* and *R31C-ICN* recipients 8 weeks post-transplant.

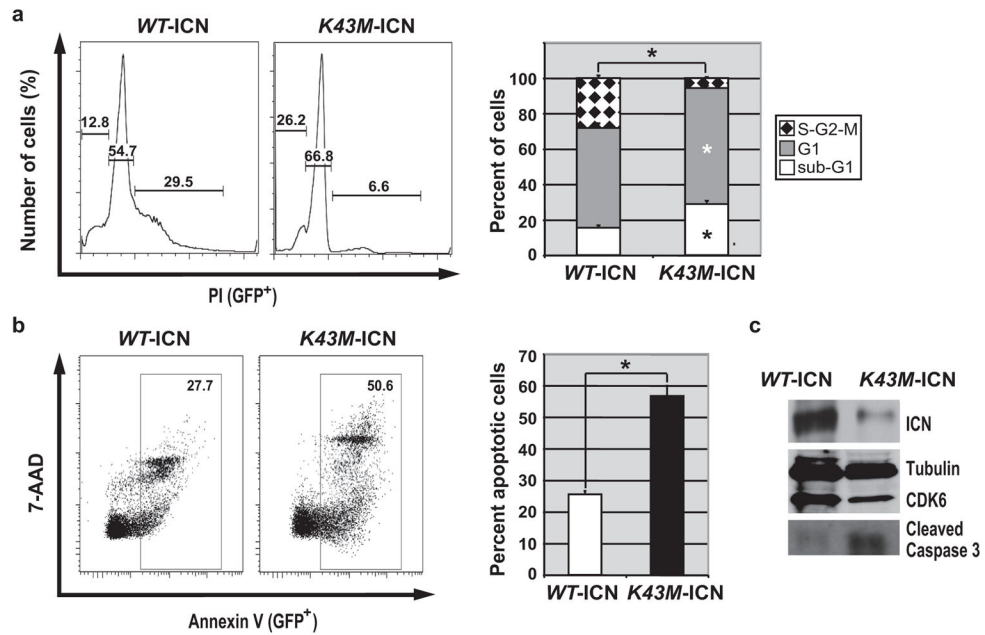


**Figure 2. Loss of CDK6 kinase activity impairs the ability of *K43M* cells to proliferate and increases apoptosis**

(a) Left panel: representative flow cytometric cell cycle profiles of GFP<sup>+</sup> cells isolated from spleen of *WT-ICN* and *K43M-ICN* recipients at 3 weeks post-transplantation. Right panel: histograms summarizing the cell cycle distribution of the cells in the left panel. Data shown are mean ± s.e. ( $n = 5$ ); \* $P < 0.05$  vs *WT-ICN*, *t*-test. (b) Left panel: representative flow cytometric profiles of apoptosis in GFP<sup>+</sup> splenocytes from *WT-ICN* and *K43M-ICN* recipients. Right panel: histograms summarizing the frequency of the apoptotic cells in the left panel. Data shown are mean ± s.e. ( $n = 5$ ); \* $P < 0.05$  vs *WT-ICN*, *t*-test. (c) Lysates from GFP<sup>+</sup> splenocytes of *WT-ICN* and *K43M-ICN* recipients harvested 3 weeks post-transplant were analyzed by immunoblotting for expression of ICN, CDK6, and cleaved Caspase 3. Tubulin was used as a loading control.



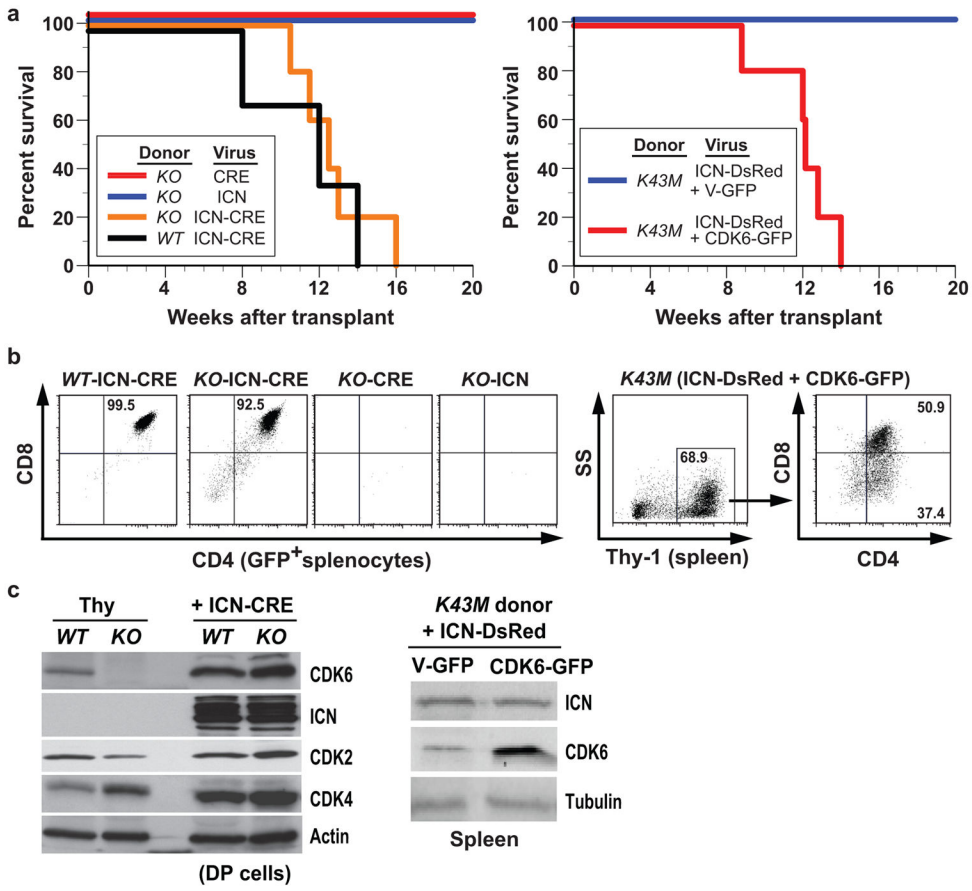


**Figure 3. Re-expression of CDK6 in *KO*/*K43M* LK cells rescues the leukemogenesis defect** (a) Left panel: Kaplan-Meier survival curves for recipients of different LK donors (*WT*, *KO*) transduced with retrovirus expressing ICN with GFP (ICN) or ICN with GFP-CRE (ICN-CRE). Survival of recipients of *KO*-CRE ( $n = 3$ ), *KO*-ICN ( $n = 7$ ), *KO*-ICN-CRE ( $n = 5$ ), and *WT*-ICN-CRE ( $n = 3$ ) is displayed. The difference in survival between *KO*-ICN-CRE and *KO*-ICN or between *KO*-ICN-CRE and *KO*-CRE recipients was significant ( $P < 0.05$ , log-rank tests). Right panel: Kaplan-Meier survival curves for recipients of *K43MLK* cells transduced with ICN-DsRed+CDK6-GFP viruses ( $n = 10$ ) and *K43MLK* cells transduced with ICN-DsRed+V-GFP viruses ( $n = 10$ ). The survival of *K43M*(ICN-DsRed+CDK6-GFP) and *K43M*(ICN-DsRed+V-GFP) recipients was significantly different ( $P < 0.05$ , log-rank test). (b) Left panel: CD4<sup>+</sup>CD8<sup>+</sup> DP cells in the GFP<sup>+</sup> splenocyte population from the indicated recipients. Right panel: splenocytes from representative recipients of *K43M* LK cells transduced with ICN-DsRed+CDK6-GFP retrovirus were analyzed for expression of Thy1 (left panel) and subsequently for CD4/8 (right panel). (c) Left panel: lysates from CD4<sup>+</sup>CD8<sup>+</sup> DP leukemia cells ( $3 \times 10^6$ ) were analyzed by immunoblotting for expression of CDK6, ICN, CDK2, and CDK4. Lysates from *WT* and *KO* thymocytes were used as controls for CDK6 expression, while actin was used as a loading control. Right panel: splenocytes from recipients of *K43M*ICN-DsRed+V-GFP or *K43M*ICN-DsRed+CDK6-GFP LK cells were lysed and analyzed by immunoblotting for CDK6 and ICN expression. Tubulin was used as loading control.

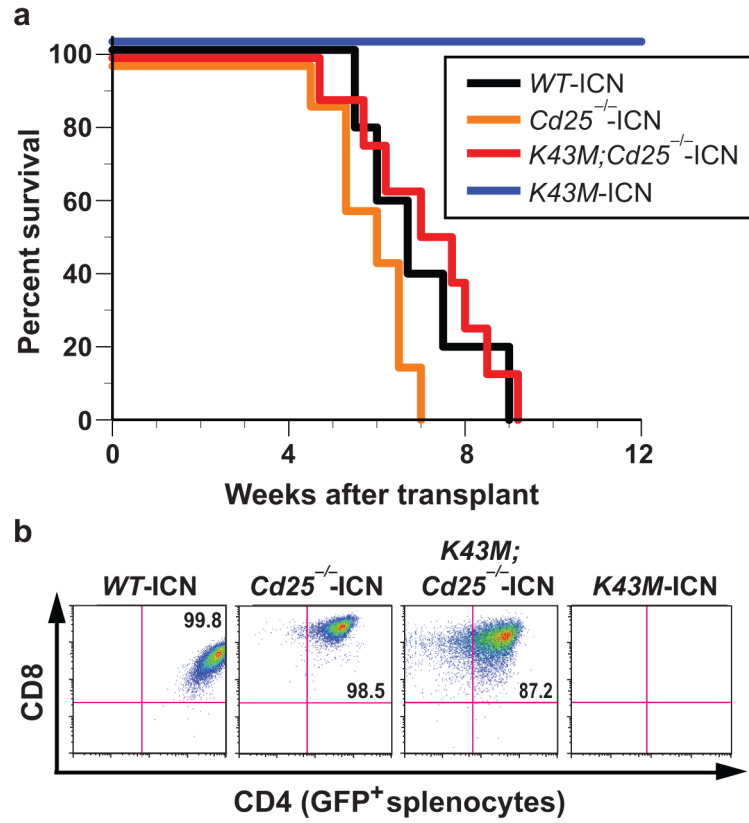


**Figure 4. Ablation of *Cd25* in the *K43M* background rescues Notch transformation**  
**(a)** Kaplan-Meier survival curves for recipients of ICN-GFP-transduced LK cells from BM of *WT* ( $n = 5$ ), *Cd25*<sup>-/-</sup> ( $n = 7$ ), *K43M*;*Cd25*<sup>-/-</sup> ( $n = 8$ ), and *K43M* ( $n = 5$ ) donors. The difference in survival between *K43M*-ICN and *K43M*;*Cd25*<sup>-/-</sup>-ICN recipients, *K43M*-ICN and *WT*-ICN recipients, and *K43M*-ICN and *Cd25*<sup>-/-</sup>-ICN recipients was significant ( $P < 0.05$ , log-rank test). **(b)** Flow cytometric analysis of CD4<sup>+</sup>CD8<sup>+</sup> DP cells in the GFP<sup>+</sup> splenocyte population from the indicated recipients. Right panel: flow cytometric analysis of CD4<sup>+</sup>CD8<sup>+</sup> DP cells in the GFP<sup>+</sup> splenocyte population from the indicated recipients.

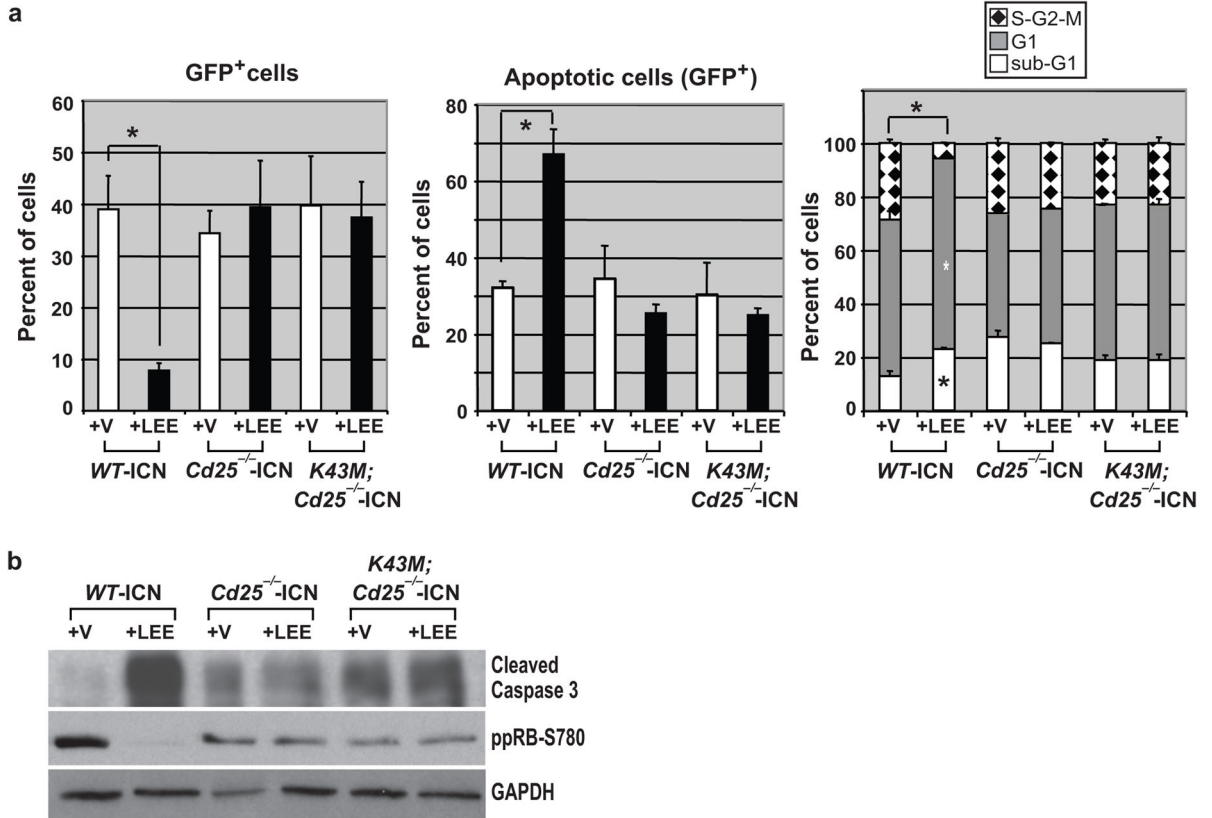


**Figure 5. Loss of CD25 protects leukemic cells from apoptosis and cell cycle arrest induced by inhibition of CDK6 kinase activity**

(a) Left panel: histograms summarizing frequency of circulating GFP<sup>+</sup> cells in WT-ICN, Cd25<sup>-/-</sup>-ICN, and K43M;Cd25<sup>-/-</sup>-ICN recipients after 7 days treatment with vehicle (+V) or LEE011 (+LEE). Middle panel: Histograms summarizing apoptosis in circulating leukemic cells isolated from WT-ICN, Cd25<sup>-/-</sup>-ICN, and K43M;Cd25<sup>-/-</sup>-ICN recipients after 7 days treatment with (+V) or (+LEE). Right panel: Histograms summarizing the cell cycle distribution of GFP<sup>+</sup> cells isolated from spleen of WT-ICN, Cd25<sup>-/-</sup>-ICN, and K43M;Cd25<sup>-/-</sup>-ICN recipients after 7 days treatment with (+V) or (+LEE). Data shown are mean ± s.e. (n = 5). \*P < 0.05 vs WT-ICN, t-test. There was no significant difference between V and LEE011 treated Cd25<sup>-/-</sup>-ICN or K43M;Cd25<sup>-/-</sup>-ICN recipients. (b) Lysates from splenocytes of WT-ICN, Cd25<sup>-/-</sup>-ICN, and K43M;Cd25<sup>-/-</sup>-ICN recipients after 7 days treatment with vehicle (+V) or LEE011 (+LEE) were analyzed by immunoblotting for expression of cleaved Caspase 3 and ppRb-S780. GAPDH was used as a loading control.

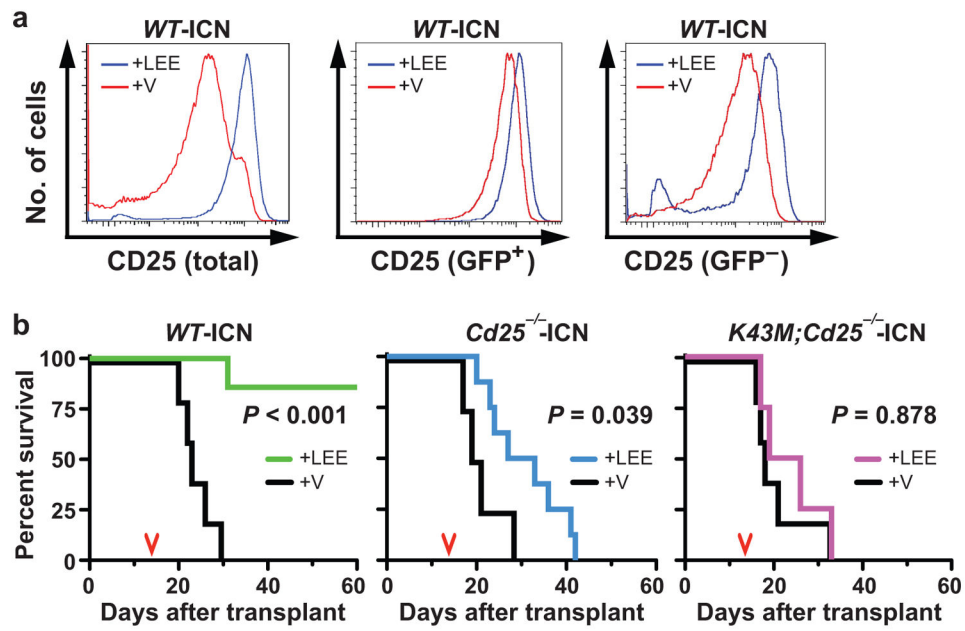


**Figure 6. CDK6-dependent suppression of CD25 mediates the therapeutic response to CDK6 inhibition in established T-ALL**

(a) Histograms comparing CD25 expression in total leukocytes (left panel), GFP<sup>+</sup> leukemic cells (middle panel), and GFP<sup>-</sup> cells (right panel) isolated from peripheral blood of *WT*-ICN recipients after 7 days treatment with vehicle (+V) or LEE011 (+LEE). (b) Kaplan-Meier survival curves for recipients of *WT*-ICN treated with vehicle (V;  $n = 9$ ) vs *WT*-ICN treated with LEE011 (LEE;  $n = 8$ ) (left panel), *Cd25*<sup>-/-</sup>-ICN-V vs *Cd25*<sup>-/-</sup>-ICN-LEE (middle panel), and *Cd25*<sup>-/-</sup>;*K43M*-ICN-V vs *Cd25*<sup>-/-</sup>-ICN-LEE (right panel).  $P$  values are listed on each panel (log-rank test comparing V- vs. LEE-treated mice). Drug treatment was initiated on d14 post-transplantation (red arrowheads) and continued until all mice in the cohort were sacrificed or for 60 days.

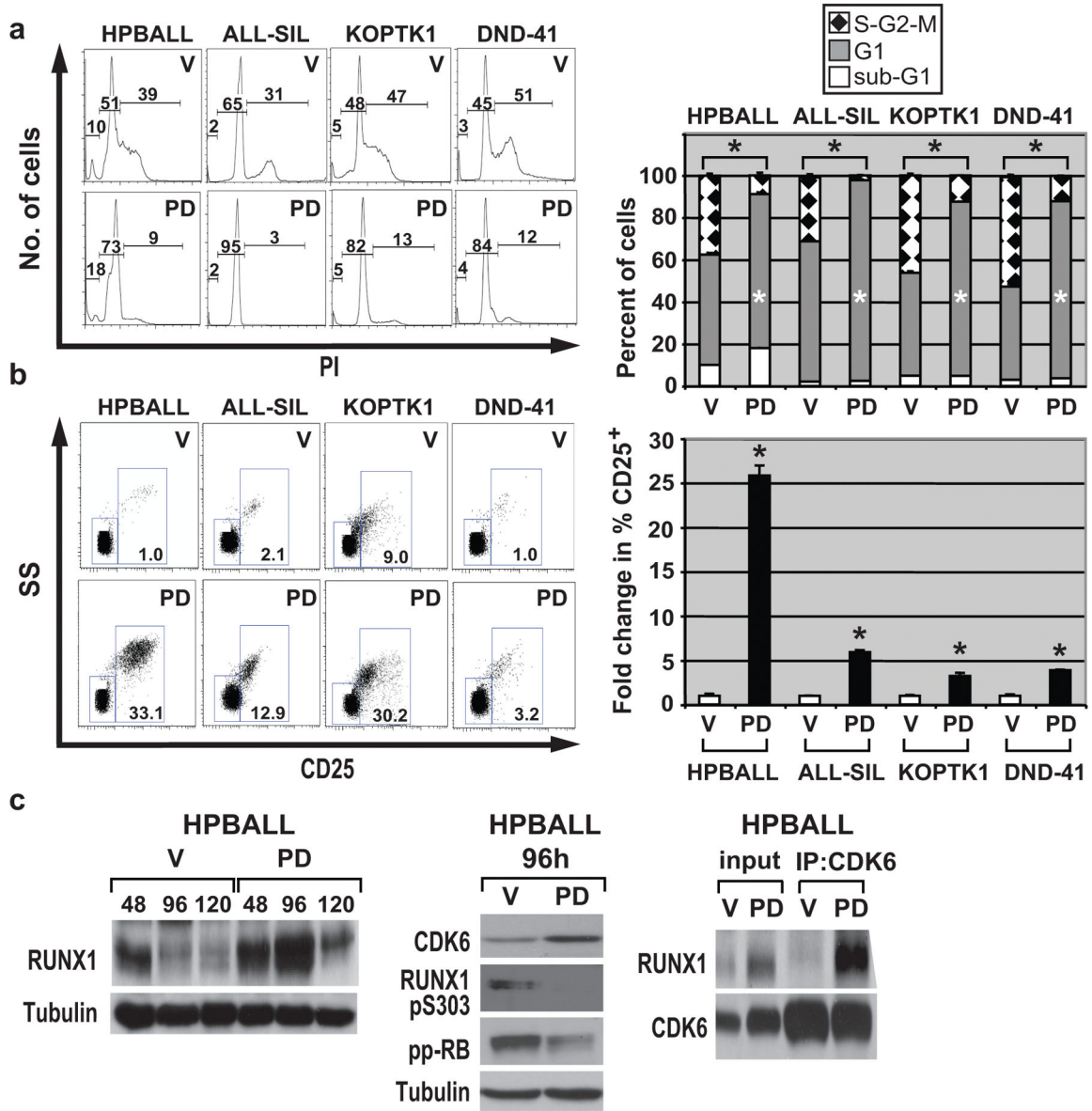


**Figure 7. Inhibition of CDK6 kinase activity leads to cell cycle arrest and up-regulation of CD25 and RUNX1 in human T-ALL**

(a) Left panel: representative cell cycle profiles of human T-ALL cell lines with Notch mutations treated with DMSO vehicle (V) or PD0332291 (PD; 0.5  $\mu$ M) for 5 days. Right panel: histograms summarizing the cell cycle distribution of the T-ALL cell lines in the left panel. Data shown are mean  $\pm$  s.e. ( $n = 4$ );  $*P < 0.05$  vs DMSO control,  $t$ -test. (b) Left panel: representative flow cytometric profiles of CD25<sup>+</sup> cells in human T-ALL cell lines treated with DMSO vehicle or PD (0.5  $\mu$ M) for 5 days. Right panel: histograms summarizing the percentage of CD25<sup>+</sup> cells in 4 different cell lines treated with DMSO vehicle or PD (0.5  $\mu$ M) for 5 days in the left panel. The percentage of CD25<sup>+</sup> cells in each line was normalized to its vehicle control, which was arbitrarily set to 1. Data shown are mean  $\pm$  s.e. ( $n = 4$ );  $*P < 0.05$  vs vehicle,  $t$ -test. (c) Left panel: representative immunoblots

showing the time course of RUNX1 expression in HPBALL cells following treatment with DMSO vehicle or PD. Tubulin was used as loading control. Middle panel: Immunoblots showing the expression of CDK6, RUNX1-pS303, and ppRB-pS780 in HPBALL cells treated with vehicle or PD for 96 hr. Right panel: CDK6 was immunoprecipitated with antibody from extracts of HPBALL cells treated with vehicle or PD, and the blots were probed with the indicated antibodies against RUNX1 and CDK6. “Input” represents the amount of extract (50  $\mu$ g) subjected to immunoblotting.

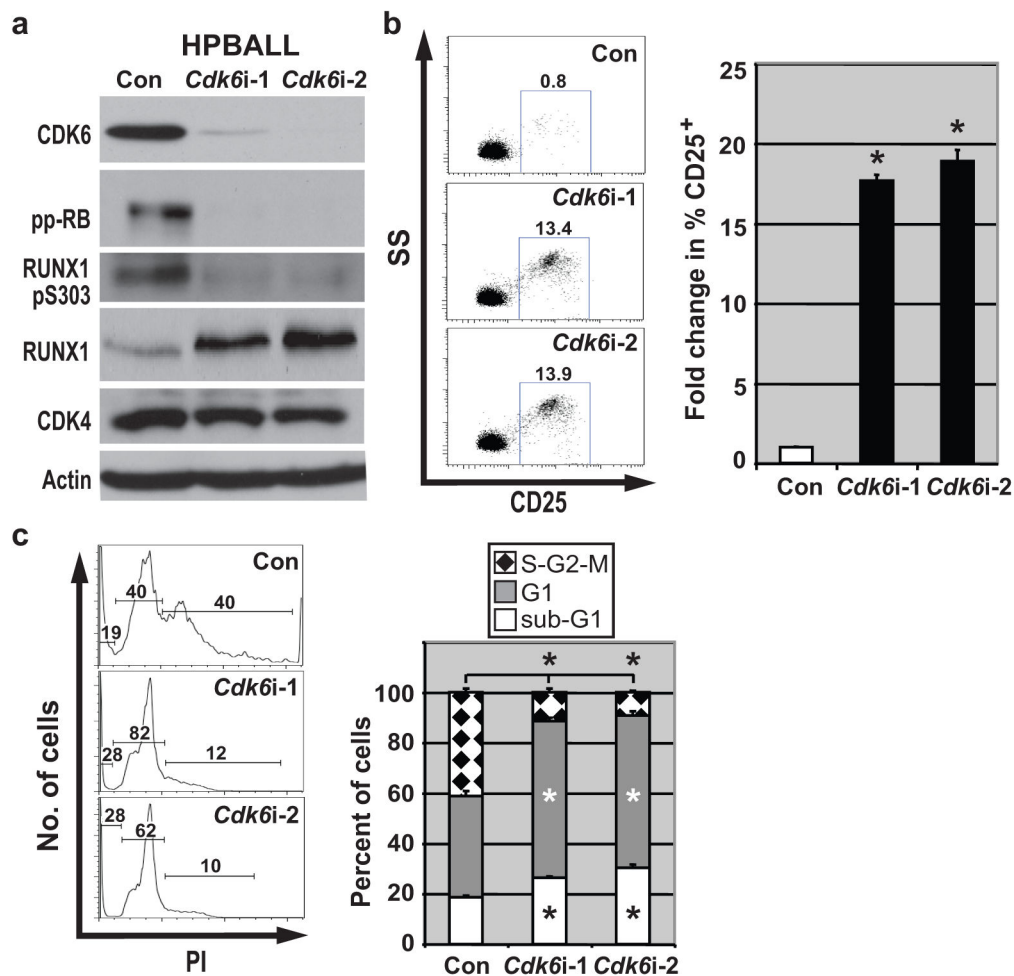


**Figure 8. *Cdk6-ShRNAs*-mediated knock-down of CDK6 leads to up-regulation of RUNX1, CD25, and cell cycle arrest in human T-ALL**  
 (a) Immunoblot analyses of CDK6, pRB-pS780, RUNX1-pS303, RUNX1, and CDK4 in HPBALL cells subjected to *Cdk6-ShRNA* (*Cdk6i-1, 2*)-mediated knockdown of CDK6. CTRL indicates a scrambled *Cdk6-shRNA* used as control. Actin was used as loading control. (b) Left panel: representative flow cytometric profiles of CD25<sup>+</sup> cells in CTRL or *Cdk6* knockdown HPBALL cells. Right panel: histograms summarizing the percentage of CD25<sup>+</sup> HBALL cells (from the left panel) normalized to control (CTRL) which was arbitrarily set to 1. Data shown are mean ± s.e. (*n* = 3 independent experiment); \**P* < 0.05 vs CTRL, *t*-test. (c) Left panel: representative cell cycle profiles of HPBALL cells following CTRL or *Cdk6-shRNA*-mediated knockdown of CDK6. Right panel: histograms summarizing the cell cycle distribution of the HPBALL cell lines in the left panel. Data shown are mean ± s.e. (*n* = 3); \**P* < 0.05 vs CTRL, *t*-test.